

# Journal of Materials Chemistry C

Accepted Manuscript



This is an *Accepted Manuscript*, which has been through the Royal Society of Chemistry peer review process and has been accepted for publication.

*Accepted Manuscripts* are published online shortly after acceptance, before technical editing, formatting and proof reading. Using this free service, authors can make their results available to the community, in citable form, before we publish the edited article. We will replace this *Accepted Manuscript* with the edited and formatted *Advance Article* as soon as it is available.

You can find more information about *Accepted Manuscripts* in the [Information for Authors](#).

Please note that technical editing may introduce minor changes to the text and/or graphics, which may alter content. The journal's standard [Terms & Conditions](#) and the [Ethical guidelines](#) still apply. In no event shall the Royal Society of Chemistry be held responsible for any errors or omissions in this *Accepted Manuscript* or any consequences arising from the use of any information it contains.

Cite this: DOI: 10.1039/c0xx00000x

www.rsc.org/xxxxxx

PAPER

# Functionalization of CdSe semiconductor nanocrystals with organic charge-transporting ligands

Yichen Liang, Jong-Sik Moon, Ruipu Mu and Jeffrey G. Winiarz<sup>a</sup>

Received (in XXX, XXX) Xth XXXXXXXXXX 20XX, Accepted Xth XXXXXXXXXX 20XX

DOI: 10.1039/b000000x

Abstract: [1,1'-Biphenyl]-4,4'-diamine-N,N'-bis(3-methylphenyl)-N,N'-diphenyl (TPD), a well-studied hole transporting material, has been sulfonated using acetyl sulfate and subsequently used as a passivating ligand in the synthesis of CdSe quantum dots (QDs). It is further demonstrated that QDs synthesized through this approach are able to serve as efficient photosensitizers in photoconductive (PC) inorganic/organic hybrid composites. Fourier-transform infrared spectroscopy confirms that the sulfonate group has been bonded to the TPD molecule. UV/visible absorption and photoluminescence (PL) spectroscopy of the sulfonated TPD (STPD) indicate that sulfonation does not significantly alter the electronic properties of TPD. Furthermore, mass spectrometry shows STPD is primarily mono-sulfonated. The STPD capped CdSe QDs (STPD-QCdSe) clearly exhibit the effect of quantum confinement in their UV/visible absorption spectra. The PL spectra of STPD-QCdSe suggest the STPD is attached to the surface of QCdSe. The morphology of STPD-QCdSe has been studied using transmission electron microscopy. The results indicate the STPD-QCdSe are approximately spherical with diameters of [3.1, 3.9] nm and highly crystalline. To demonstrate the enhancement in charge-transfer efficiency associated with STPD-QCdSe, two types of PC composites were fabricated. The first was photosensitized through the inclusion of STPD-QCdSe, and the other included CdSe QDs capped with trioctylphosphine (TOPO-QCdSe), with molecular TPD serving as the charge transport matrix in both cases. The PC was measured as a function of the external electric field,  $E$ , with the PC of the composite sensitized with STPD-QCdSe exceeding that of the composite sensitized with TOPO-QCdSe by a factor of  $\sim 15$  with  $E = 10 \text{ V}/\mu\text{m}$ .

## Introduction

Semiconductor nanocrystals, also known as quantum dots (QDs) have aroused tremendous interest in fields concerning optical and electro-optic applications due to their unique properties (e.g. tunable absorption, narrow photoemission, etc.).<sup>1</sup> Currently QDs have been successfully applied in the manufacturing of photodetectors,<sup>2</sup> solar cells,<sup>3</sup> light emitting diodes<sup>4</sup> and field effect transistors.<sup>5</sup> In the past several decades, there has been significant progress in the methods used in the synthesis of QDs with solution-based colloidal synthesis being one of the most commonly employed techniques. Solution-based colloidal syntheses are relatively facile techniques that can produce QDs with controllable size and few crystalline defects. The QDs synthesized using these methods are often passivated with capping ligands consisting of an anchoring end group, e.g. thiol, amino-, carboxylic, etc., attached to a hydrocarbon chain. Due to the presence of hydrocarbon chain, these commonly employed ligands are electrically insulative in nature, thus hindering their use in applications relying on a charge-transfer process between the QDs and any conductive matrix in which the QDs are

contained.<sup>6,7</sup> Different techniques have been investigated in an effort to eliminate the insulative layer, including the exchange of the long hydrocarbon capping ligands with smaller ligands (e.g. pyridine),<sup>8</sup> chemically removing the capping ligands by treating the QDs with sodium hydroxide<sup>9</sup> and hydrazine,<sup>5</sup> and heat annealing.<sup>10</sup> None of these techniques, however, can completely remove the insulating shell and, in most cases, the stability of the QDs is adversely affected. For these reasons it is desirable to synthesize the QDs directly in the presence of a passivating ligand which lends itself to the charge-transfer process.

The hole transporting material, [1,1'-Biphenyl]-4,4'-diamine-N,N'-bis(3-methylphenyl)-N,N'-diphenyl (TPD) is well-studied and has been widely used in both electronic and electro-optic devices.<sup>11</sup> Due to its  $\pi$ -stacking structure<sup>12</sup> and molecular conformation,<sup>13</sup> TPD exhibits a hole mobility of  $\sim 10^{-3} \text{ cm}^2/(\text{Vs})$  under an externally applied electric field,  $E$ , of below  $1 \text{ V}/\mu\text{m}$ ,<sup>12</sup> an extremely high figure-of-merit among organic hole transporting materials. However, due to its lack of appropriate functional groups, it is unable to act as a passivating group in the synthesis of QDs. In this article, a novel technique for the appropriate functionalization of TPD and the subsequent

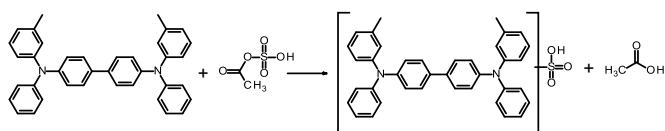


Fig. 1 Sulfonation reaction for TPD.

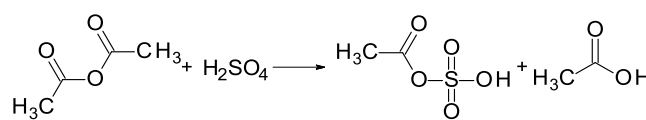


Fig. 2 The synthesis reaction of acetyl sulfate.

passivation of CdSe semiconductors nanocrystals (QCdSe) is reported. Here, the TPD was modified through the covalent bonding of a sulfonate group to one of the phenyl groups located on the TPD molecule resulting in sulfonated TPD (STPD), as illustrated in Fig 1. Acetyl sulfate was selected as the sulfonation agent due to its relatively mild nature compared with more typical sulfonating agents such as sulfuric acid, which may degrade the TPD. Hence, whereas the pristine TPD lacks affinity for the surface of the QCdSe, the functionalized TPD molecule readily associates with the surface of QCdSe due to the presence of the electron-rich sulfonate group. The STPD was characterized using UV/visible spectroscopy, photoluminescence (PL) spectroscopy, Fourier-transform infrared (FTIR) spectroscopy and mass spectrometry (MS).

The STPD was subsequently used as the surfactant/passivating ligand in the synthesis of QCdSe passivated with STPD ligands (STPD-QCdSe) in a facile, room temperature reaction, appropriately modified from that found in the literature.<sup>14</sup> The procedure on which this technique is based employed sulfonated polyvinyl carbazole (PVK) to synthesize QCdS.<sup>14</sup> Compared with PVK, TPD is reported to have higher charge drift mobility.<sup>15</sup> Hence, it is anticipated that TPD-based composites should demonstrate superior photoconductive (PC) properties. The STPD-QCdSe was characterized using UV/visible and PL spectroscopy, as well as transmittance electron microscopy (TEM).

PC experiments were conducted to evaluate any improvement in charge-transfer efficiency of STPD-QCdSe relative to that of QCdSe passivated with a more traditional passivating agent, trioctylphosphine (TOPO) in this case. Two types of PC samples were fabricated using TPD as the charge-transport matrix; one type photosensitized with STPD-QCdSe and the other type photosensitized with TOPO capped QCdSe (TOPO-QCdSe). The STPD-QCdSe and the TOPO-QCdSe were synthesized such that they possessed band-gap energies of similar magnitude, corresponding to a wavelength of  $\lambda \approx 540\text{nm}$ . The PC experiments were conducted using Helium Neon laser operating at  $\lambda = 543\text{ nm}$ .

## Experiment

### Chemicals

TPD was purchased from Magical Scientific Corporation. Cadmium acetate dihydrate, selenium powder (100 mesh, 99.99%), sodium borohydride (98%), acetic anhydride (99+%), 1-butanol (99.9%) and 1,2-dichlorobenzene (99% reagent plus) were purchased from Sigma Aldrich Corporation. Sulfuric acid (95%-98%) was purchased from Alfa Aesar Corporation. All chemicals were used as received. Deionized (DI) water was produced using an Advantage A 10 Mili-Q system from Millipore Corporation.

### Sulfonation of TPD

The sulfonation agent, acetyl sulfate, was prepared based on a method described in literature<sup>16</sup> with minor modifications. Here, acetic anhydride (0.38 ml) was dissolved in 2 ml of chloroform and stored in an ice bath for 5 min after which 0.14 ml of 96% sulfuric acid was added dropwise. At temperatures lower than 10 °C, acetyl sulfate is formed by the process illustrated in Fig. 2.<sup>16</sup> The final concentration of the prepared acetyl sulfate solution was 1 M and was used at this concentration in the subsequent sulfonation of TPD.

For the sulfonation of TPD, 50 mg of TPD was dissolved in a 20 ml glass vial containing 1 ml chloroform and placed in an ice bath. After 20 min, 150  $\mu\text{l}$  of the prepared acetyl sulfate solution was added to the TPD/chloroform solution dropwise under strong magnetic stirring and the final mixture was placed in a temperature controlled vacuum oven with a temperature of  $\sim -5^\circ\text{C}$ . The chloroform and acetic acid byproducts were removed gradually under vacuum. The removal of acetic acid shifted the reaction toward the products, thus increasing the STPD yield. Upon removal of the solvent, the reaction vial was kept under vacuum for an additional 5 hr to remove residual acetic acid, finally yielding a light yellow powder. The reaction process is depicted in Fig. 1.

### Characterization of STPD

Spectroscopic techniques including UV/visible spectroscopy, PL spectroscopy and FTIR spectroscopy as well as mass spectrometry were used to analyze both pristine TPD and STPD. The UV/visible spectroscopic characterization was conducted using a Cary 50 UV/visible spectrophotometer with TPD and STPD dissolved in a mixture of chloroform/butanol (3:1 by volume) at the same concentration of 0.01 mM. A quartz cuvette produced by Fisher Scientific Corporation was used as the sample cell.

PL characterization was conducted using a LS-5 Fluorescence Spectrophotometer produced by Perkin-Elmer Corporation. Samples were excited by a 330 nm light source. The same quartz cuvette used in the UV/visible spectroscopy was used in this PL spectroscopic analysis. The concentration of the analyte in each case was 0.01 M. No additional purification was conducted for the synthesized STPD prior to UV/visible or PL spectroscopic characterization.

For FTIR spectroscopic and mass spectrometric characterizations, STPD samples were purified by column chromatography using chloroform/methanol (2:1 by volume) as the elution phase. The FTIR spectra were taken using a Nexus 470 FT-IR spectrometer. The TPD and STPD samples used for FTIR were solvent cast on a sodium chloride pellet using chloroform/butanol (3:1 by volume).

Mass spectrometry measurements were conducted on an AB Sciex 4000 Q trap MS/MS system. The purified STPD samples

were dissolved in methanol and injected into the spectrometer using the infusion technique. Negative mode was employed.

### Synthesis of QCDSe using STPD Ligands

For the synthesis of STPD-QCdSe, 50 mg of TPD was sulfonated and used without additional purification. The STPD was dissolved in 4 ml chloroform/ethanol (1:1 by volume) forming a light-yellow solution. Sodium hydrogen selenide was prepared according to the steps described in literature<sup>17</sup> with minor modifications. Here, nitrogen gas was bubbled through 1.5 ml DI H<sub>2</sub>O mixed with 1 ml ethanol under strong magnetic stirring for 5 min at room temperature to remove any dissolved oxygen. Subsequently, sodium borohydride (11.5 mg, 0.305 mmol) was dissolved into the solution. Selenium powder (11.5 mg, 0.145 mmol) was then added to the solution. A significant amount of foaming due to the evolution of H<sub>2</sub> was observed. The selenium powder was consumed within 10 min. The ensuing sodium hydrogen selenide stock solution was transparent and colorless and used for STPD-QCdSe synthesis without further processing. Different sized STPD-QCdSe were produced by varying the synthesis temperature. STPD-QCdSe labeled as 1, 2 and 3 were synthesized at temperatures of 20° C, 0° C and -15° C, respectively. For the synthesis, 75  $\mu$ l of cadmium acetate dihydrate stock solution (0.02 mg/ml) was added to the STPD solution under magnetic stirring at room temperature. Subsequently, 110  $\mu$ l of the prepared sodium hydrogen selenide stock solution was swiftly injected into the mixture. The reaction occurred almost immediately, as indicated by the lightening in the color of the mixture. Simultaneously, a red precipitate, later verified as STPD-QCdSe, appeared in the solution. The precipitate was separated from the reaction mixture by centrifuging for 20 s. The liquid phase containing excess STPD was discarded and the precipitate was dispersed in 1 ml of 1,2-dichlorobenzene. To remove excess TPD, STPD, and STPD that may have been only loosely associated with the QCdSe cores, 0.5 ml of methanol was added to the STPD-QCdSe/dichlorobenzene suspension precipitating the STPD-QCdSe. The solvent was discarded and the precipitated STPD-QCdSe was redispersed in dichlorobenzene. This precipitation/redispersion procedure was repeated three times. The STPD-QCdSe suspensions 1, 2, and 3 had dark red, red and orange color, respectively, with no visible scattering. QCdSe synthesized using this procedure, but without the addition of STPD, resulted in a brown product which could not be dispersed in any common solvent. This strongly indicates that the surfaces of the STPD-QCdSe are effectively passivated with the organic STPD ligands. The STPD-QCdSe/dichlorobenzene colloidal suspensions were stored for further characterization.

### Nanocrystal Characterization

The synthesized STPD-QCdSe was characterized using UV/visible spectroscopy, PL spectroscopy and TEM. Spectroscopic characterizations were conducted on the same instruments used for STPD characterizations. For UV/visible spectroscopy, STPD-QCdSe with different particle sizes were dissolved in 1,2-dichlorobenzene. For PL spectroscopy characterization, STPD-QCdSe3 was dissolved in 1,2-dichlorobenzene. Similar concentrations of  $\sim 5 \times 10^{-6}$  M were used in acquiring the UV/visible and PL spectra. As a comparison, the PL

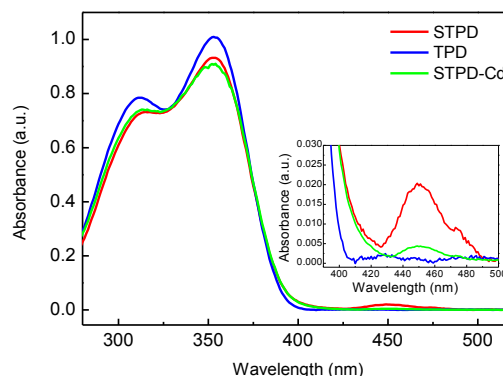


Fig. 3 UV/visible absorbance spectra of TPD and STPD.

spectrum of STPD solution after adding cadmium acetate was also acquired. A Tecnai F20 STEM, operated at 200 kV, was used for TEM characterizations. To analyze its chemical composition, energy dispersive spectroscopy (EDS) was also conducted on the STPD-QCdSe samples. The TEM sample was prepared by placing a drop of diluted dichlorobenzene dispersed STPD-QCdSe3 onto a 300 mesh copper grid. The copper grid, coated with a lacey carbon film, was purchased from Electron Microscopy Science Corporation.

### Photoconductivity analysis

PC characterizations were conducted using a DC photocurrent technique where a Keithley electrometer was used to measure the current passing through the sample as a function of  $E$ . PC samples were fabricated by sandwiching the PC composite between two ITO coated glass plates with a thickness of 10  $\mu$ m controlled by glass spacers. For this study, four PC composites were fabricated. Devices 1, 2 and 3 were photosensitized with STPD-QCdSe1, 2, and 3, respectively, and device 4 was photosensitized with TOPO-QCdSe. The concentrations of the photosensitizers were adjusted to achieve an absorbance of  $\sim 10$   $\text{cm}^{-1}$  at the excitation wavelength. The weight percentages of photosensitizers in devices 1 - 4 are 0.38 %, 0.39 %, 0.40 % and 0.40 %, respectively. All PC devices used TPD as the charge-transport matrix. The absorption spectra of devices 1 - 4 were acquired using the same spectrophotometer for STPD characterization. The PC experiments were conducted using helium-neon laser operating at the wavelength  $\lambda = 543$  nm. The incident beam intensity is 2.31 mW. Both photoconductivity,  $\sigma_p$ , and dark conductivity,  $\sigma_d$ , were calculated using the equation  $\sigma = J/E$ , where  $J$  is the experimentally determined current density.

## Results and discussion

### Characterization of STPD

Fig. 3 illustrates the UV/visible absorption spectra of TPD, STPD and STPD-Cd conjugate (the result of reacting the STPD with the Cd precursor void of Se precursor), in chloroform/butanol (3:1 by volume). Evident in the figure, the absorption spectra of STPD is very similar to that of pristine TPD. The greatest difference lies in the region from roughly 300 to 380 nm. Here, the shoulder seen

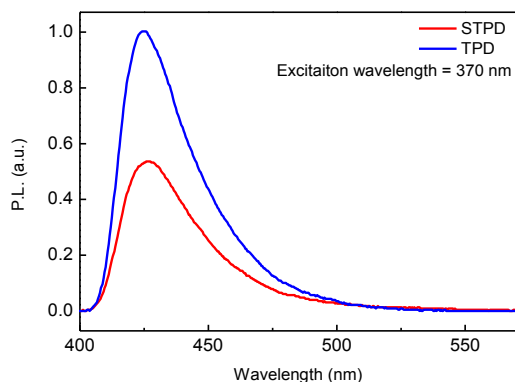


Fig. 4 PL spectra of TPD and STPD

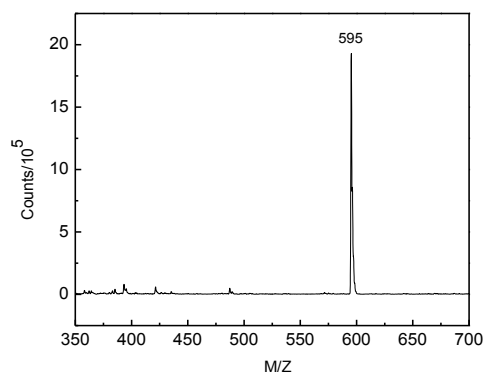


Fig. 6 Mass spectrum of STPD under negative mode.

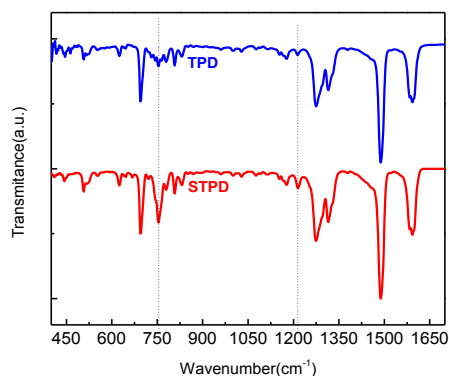


Fig. 5 FTIR spectra of TPD and STPD. The dashed lines designate the additional peaks attributed to the  $-\text{SO}_3\text{H}$  group in STPD.

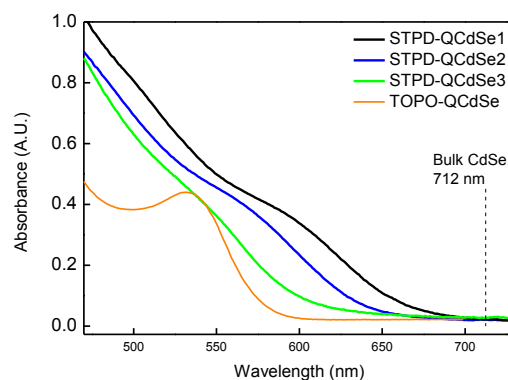


Fig. 7 UV/visible spectra of STPD-QCdSe1, 2 and 3, and TOPO-QCdSe.

in the TPD spectrum at  $\sim 320$  nm becomes slightly less pronounced after sulfonation. Additionally, within the range of roughly 400 nm and 480 nm, there is a small increase in the absorption of STPD relative to that of TPD, which likely accounts for the light-yellow color of the STPD solution. Because the absorption peaks for TPD and STPD are at nearly the same position, it is likely that the band-gap was not significantly altered by the sulfonation process. The magnitudes of absorption for TPD and STPD at their respective maxima ( $\sim 360$  nm) were also comparable. These similarities indicate the sulfonation process did not significantly affect the electronic structure associated with TPD. With these results in mind, it is anticipated that the STPD will retain its potential for efficient charge transfer, integral to the intended application of passivating QCdSe for use as a photosensitizer in PC composites.

Fig. 4 illustrates the PL spectra of TPD and STPD. The PL peaks are located at approximately the same position ( $\sim 430$  nm). However, the PL quantum efficiency of STPD is reduced compared to that of TPD, indicating that the sulfonation process results in a non-radiative energy dissipation path in addition to the PL radiative process. Again, the PL spectra imply that sulfonation did not significantly modify the electronic structure of TPD.

FTIR spectroscopy was also used to characterize the STPD and the spectra of TPD and STPD are shown in Fig. 5. Compared to pristine TPD, the spectrum of STPD exhibits two additional peaks at  $755\text{ cm}^{-1}$  and  $1215\text{ cm}^{-1}$  which can be attributed to the S-O and S=O bond stretching vibrations, respectively.<sup>18</sup> With the exception of the newly observed peaks, no additional significant differences were identified. These data indicate that  $-\text{SO}_3\text{H}$  has been successfully linked to the TPD molecule void of additional changes in the TPD structure.

Finally, MS spectrometry was used to characterize the synthesized STPD and is illustrated in Fig. 6. Only one intense peak at  $M/Z = 595$ , corresponding to mono-sulfonated STPD, is present in the spectrum. The reason for the mono-sulfonated TPD occurring as the major products is rationalized as follows. When the initial sulfonate group has bonded to the TPD molecule, the conjugated electrons associated with the TPD molecule were shifted towards the electronegative sulfur atom in the sulfonate group, ultimately deactivating the TPD from any further reaction with the acetyl sulfate.

#### Characterization of STPD-QCdSe

Fig. 7 illustrates the UV/visible absorption spectra of STPD-QCdSe. Because the STPD has no appreciable absorption in the range between 500 and 650 nm, the observed spectral features

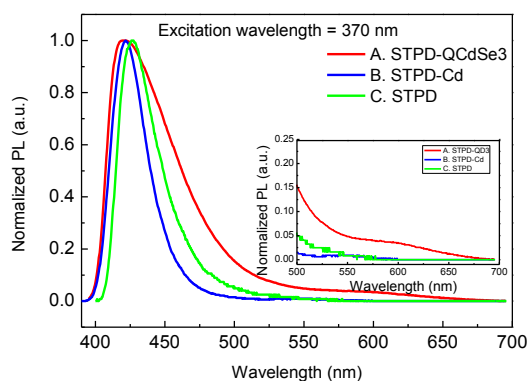


Fig. 8 PL spectra of STPD and STPD-QCdSe3.

can be attributed to the CdSe component of the STPD-QCdSe. The band-gap of bulk CdSe is also indicated in the figure. In all three STPD-QCdSe, the location of the peak associated with the first exciton is blue-shifted relative to that of bulk CdSe, clearly showing the effects of quantum confinement. The spectra of STPD-QCdSe do not exhibit a sharp peak, but rather a relatively broad shoulder in the range from 500 nm to 600 nm. This feature indicates that the STPD-QCdSe have a broad particle size distribution, typical for QCdSe synthesized at low temperature.<sup>19,20</sup> For applications requiring a relatively more narrow size distribution, size selective precipitation may be used to achieve a more mono-disperse product. Also evident is that as the temperature in the synthesis of the STPD-QCdSe is decreased, the peak is increasingly blue-shifted, indicating an associated decrease in particle size. The absorption shoulder of STPD-CdSe1 occurs at ~590 nm, while the absorption of STPD-CdSe2 and STPD-CdSe3 appear near ~570 nm and ~550 nm, respectively (see Fig 7). For comparison, bulk CdSe exhibits an absorption edge at approximately 712 nm at room temperature.

The normalized PL spectrum of STPD-QCdSe3 in 1,2-dichlorobenzene is illustrated Fig. 8. For comparison, the PL spectra of STPD and STPD-Cd conjugate (the result of reacting the STPD with the Cd precursor void of Se precursor), both dissolved in chloroform/ethanol (1:1 by volume), were acquired as well. It is noted that the PL spectrum of the STPD-Cd conjugate is slightly blue shifted relative to that of STPD, signalling the successful formation of the complex. This is also supported by the observed change in color associated with the addition of cadmium acetate to the STPD solution forming the STPD-Cd complex (see Fig. 3). In addition, the primary peak, associated with the STPD ligand is significantly broadened in the range of ~425 to 525 nm and there is also the emergence of a shoulder in the range of ~525 to 675 nm. The broadening of the primary peak attributed to the STPD ligand may be caused by several factors including steric effects caused by the crowding of the STPD on the QCdSe surface, which may lead to the deformation of the molecule, hence affecting the molecular energy levels. In addition, the bonding of the STPD ligand with QCdSe may shift the STPD energy levels accordingly. The emergence of the shoulder (~525 to 675 nm) is attributed directly to the QCdSe. It is assumed that this feature is in the form of a shoulder, and not a

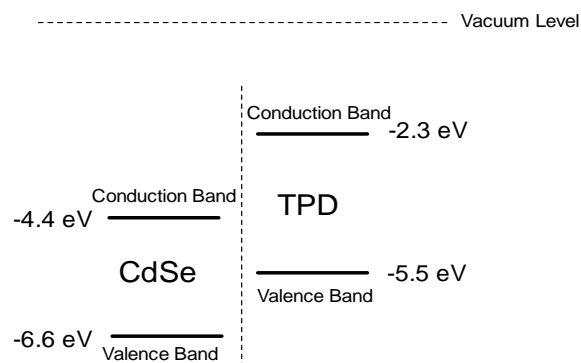


Fig. 9 VB and CB positions of TPD and CdSe

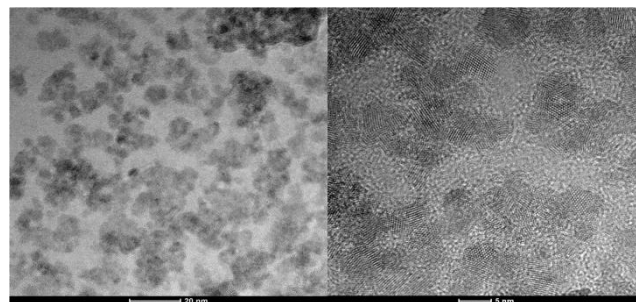


Fig. 10 TEM images of STPD-QCdSe3.

peak, due to the relatively broad size distribution associated with the QCdSe. The relatively low PL of the QCdSe can be attributed to the surface passivation with the charge transport ligands STPD. Here it is speculated that excited charge-carriers associated with the QCdSe can be transferred to the environment through the STPD ligands and subsequently trapped, rather than undergoing radiative recombination. This speculation is rationalized by consideration of the energy levels associated with TPD and CdSe, illustrated in Fig. 9.<sup>21, 22, 23</sup> While the quantum confinement effect can shift the positions of the valence band (VB) and conduction band (CB) in QCdSe, the relatively large particle size (>3 nm) of QCdSe investigated in this study indicates that the shift is less than 0.4 eV,<sup>24</sup> which can be neglected in the following comparison with TPD energy levels. As seen in the figure, it is energetically favourable for an electron which is photo-excited to the CB of QCdSe to relax into the VB of TPD, thus hindering radiative recombination. The observed reduction in STPD-QCdSe thus indicates that the STPD ligands are conjugated on the surface of QCdSe nanocrystals. Similar PL quenching was also observed in QDs passivated with sulfonated PVK.<sup>14</sup> As illustrated in Fig. 8, the PL associated with the STPD ligand is largely retained in the PL spectrum of the STPD-QCdSe (in the range from 400 nm to 480 nm). During the synthesis procedure, excess STPD which was not tethered to the surface of QCdSe was removed during the washing process. It is further noted that the addition of methanol to a STPD/1,2-dichlorobenzene solution did not result in an observable precipitate, indicating that STPD remains soluble in this solvent combination and therefore excess STPD should be removed in the washing process. Therefore, the observed STPD emission in the PL spectrum of STPD-QCdSe3 can only be attributed to STPD associated with the surface of QCdSe. This also indicates that the surface of STPD-QCdSe has

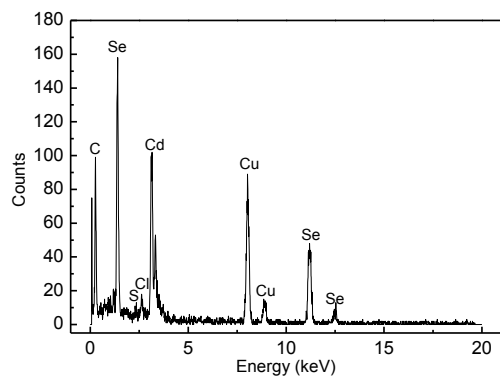


Fig. 11 EDS of STPD-QCdSe3

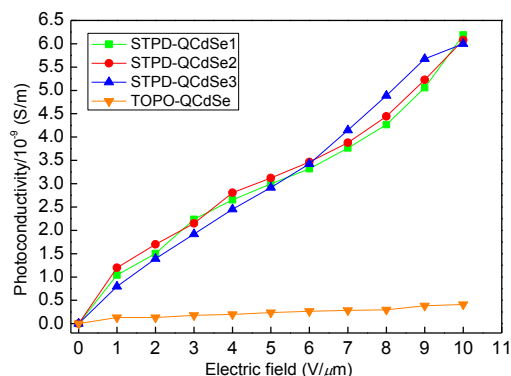


Fig. 13 Photoconductivities of composites

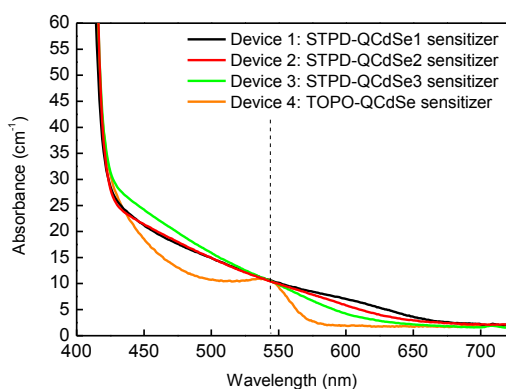


Fig. 12 Absorption spectra of active layers in PC devices

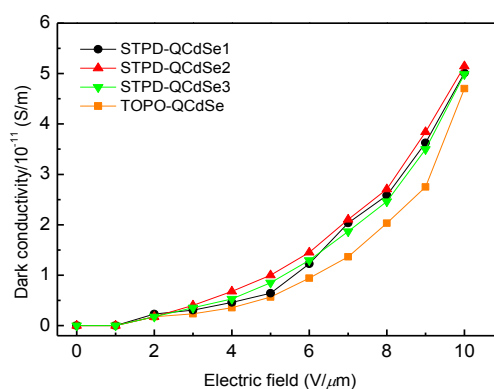


Fig. 14 Dark conductivities of composites

5 been successfully passivated with STPD.

The morphology of STPD-QCdSe3 was studied using TEM and the data are presented in Fig. 10. Evident from the figure, the QDs are roughly spherical in shape. The average particle diameter was  $3.0 \pm 0.5$  nm ( $n = 23$ ). Using 550 nm as the position of the absorption shoulder for STPD-QCdSe3 (see Figure 8), in conjunction with the empirical equation,  $D = (1.6122 \times 10^{-9}) \lambda^4 - (2.6575 \times 10^{-6}) \lambda^3 + (1.6242 \times 10^{-3}) \lambda^2 - (0.4277) \lambda + 41.57$ , where  $D$  (nm) is the diameter of QDs and  $\lambda$  (nm) is the absorption wavelength at the maximum,<sup>25</sup> the diameter of STPD-QCdSe3 was calculated to be 3.1 nm, consistent with the TEM data. By applying the same equation and using 590 nm and 570 nm as the position of absorption shoulder, the diameters of STPD-QCdSe1 and STPD-QCdSe2 were calculated as 3.9 nm and 3.5 nm, respectively. Based on the experimental and calculated data, the radii of the synthesized QDs are smaller than the Bohr radius of CdSe of 5.6 nm,<sup>26</sup> resulting in the observed quantum confinement effect seen in Fig. 8. As seen in the TEM images, the STPD-QCdSe were evenly dispersed on the TEM grid, although a small amount of aggregation existed. The aggregation may suggest that the passivation of QCdSe using STPD is not as effective as with traditional ligands e.g. TOPO. The high-resolution TEM image also reveals that the QCdSe are well crystallized. The chemical

30

composition of STPD-QCdSe3 is revealed in the EDS spectrum (Fig. 11). The peaks associated with Cd and Se elements evidently confirm the synthesized nanocrystals are CdSe. Quantified using the FEI TIA (TEM Imaging and Analysis) method, the molar ratio of Cd/Se is 55.33/44.55. The Peaks associated with Cu and C are representative of the carbon coated copper grid. The Cl-peak is attributed to residual solvent (dichlorobenzene). An S-peak exists in the spectrum which furthermore proves that STPD ligands were capped on the surface of CdSe nanocrystals.

For PC experiments, organic PC composites were fabricated using TPD as the charge-transfer matrix, while STPD-QCdSe1, 2 and 3 and TOPO-QCdSe were employed as photo-sensitizers. The TOPO-QCdSe were synthesized via a routine procedure,<sup>6</sup> with its absorption spectrum depicted in Fig. 7. The concentrations of the two types of photo-sensitizers were tailored in order to ensure the composites have a similar absorption cross-section at 543 nm, the wavelength of the excitation source. The absorption spectra of the PC devices are shown in Fig. 12.

For the photosensitization process to operate efficiently, the VB of the photosensitizer must occur lower in energy than that of the charge transporting matrix, TPD in this case. As such, upon absorption of a photon by QCdSe, an electron is promoted from

its VB to its CB, resulting in an electron and a hole in the CB and VB, respectively.<sup>21</sup> Due to the relative position of their energy levels, it is energetically favorable for an electron in the VB of TPD to relax to the VB of QcDSe. As a result, the photogenerated electrons are associated with the CB of QcDSe and the holes are associated with the VB of TPD. Because the concentration of STPD-QcDSe is ~0.4 %, well below the percolation threshold, the holes associated with the TPD matrix will be the primary charge-transporting species.

The photoconductivity and dark conductivity for the PC devices are presented in Fig. 13 and 14. The devices photosensitized with STPD-QcDSe show significantly higher PC than does the device photosensitized with TOPO-QcDSe, while the dark conductivities of them are quite similar. No significant difference in the PC between devices 1, 2 and 3 can be observed. As a control, the PC and dark conductivities were also measured for TPD, void of any photosensitizer, under the same experimental conditions. Here, no detectable PC was observed while the dark conductivity was similar to that of other devices. In device 4, the photo-sensitizing TOPO-QcDSe is encapsulated by a layer of electrically insulative TOPO. This insulative layer acts as a barrier to the charge-transfer process between the QcDSe cores and the TPD matrix. In devices 1, 2 and 3, the QcDSe are encapsulated with STPD, and because STPD is conducive to the charge-transfer process, photo-excited charges are easily transferred from the QcDSe semiconductor core, through the ligands, and ultimately to the TPD charge-transporting matrix. As a result, the PC of these devices is greatly enhanced compared to that of device 4. The dark conductivity was not significantly influenced by the presence of the photosensitizers. Additionally, because the capping ligands have a molecular structure similar to that of the matrix, STPD-QcDSe is more easily dispersed in the matrix than is TOPO-QcDSe, which may also have a positive effect over the PC characteristics of the composite.

## Conclusions

A relatively simple method for sulfonating TPD was developed and the sulfonated products can be used as passivating ligands in the synthesis of STPD-QcDSe. The sulfonated TPD is primarily mono-sulfonated. The UV-visible spectroscopy and PL spectroscopy results indicate that the sulfonation did not have a significant influence on TPD's electronic structure. The diameter of the synthesized STPD-QcDSe ranges from 3.1 to 3.9 nm and quantum confinement is observed in the UV-visible spectra. The newly developed STPD passivated QcDSe were used as a photosensitizer in STPD-QcDSe/TPD PC composites. A significant improvement in the PC of a STPD-QcDSe/TPD device was observed compared with that of a TOPO-QcDSe/TPD device (~ a factor of 15 at 10 V/ $\mu\text{m}$ ) while dark conductivity of two types of composites were nearly identical.

## Acknowledgements

This work is supported by Missouri Research Board.

## Notes and references

- <sup>a</sup> 332 Schrenk Hall, Missouri University of Science and Technology, Rolla, MO, USA. Fax: 573 341 6033; Tel: 573 341 6733; E-mail: Winiarzj@mst.edu
- D. V. Talapin, J. Lee, M. V. Kovalenko and E. V. Shevchenko, *Chem. Rev.*, 2010, **110**, 389.
  - G. Konstantatos, I. Howard, A. Fischer, S. Hoogland, J. Clifford, E. Klem, L. Levina and E. H. Sargent, *Nature*, 2006, **442**, 180.
  - E. J. D. Klem, D. D. MacNeil, P. W. Cyr, L. Levina and E. H. Sargent, *Applied Physics Letter*, 2007, **90**, 183113.
  - V.L.Colin, M. C. Schlamp and A. P. Alivisatos, *Nature*, 1994, **370**, 354.
  - D. V. Talapin and C. B. Murray, *Science*, 2005, **310**, 86.
  - S. V. Voitekhovich, D. V. Talapin, C. Klinke, A. Kornowski and H. Weller, *Chem. Mater.*, 2008, **20**, 4545.
  - N. C. Greenham, X. Peng and A. P. Alivisatos, *Physical Review. B*, 1996, **54**, 17628.
  - C. B. Murray, D. J. Noms and M. G. Bawendi, *J. Am. Chem. Soc.*, 1993, **115**, 8706.
  - M. V. Jarosz, V. J. Porter, B. R. Fisher, M. A. Kastner and M. G. Bawendi, *Physical Review B*, 2004, **70**, 195327.
  - V. J. Porter, S. Geyer, J. E. Halpert, M. A. Kastner and M. G. Bawendi, *J. Phys. Chem. C*, 2008, **112**, 2308.
  - Y. Shirota, *J. Mater. Chem.*, 2000, **10**, 1-25.
  - M. Stolka, J. F. Yanus, D. M. Pai, *J. Phys. Chem.*, 1984, **88**, 4707.
  - A. R. Kennedy, W. Ewen Smith, D. R. Tackley, W. I. F. David, K. Shankland, B. Brown and S. J. Teat, *J. Mater. Chem.*, 2002, **12**, 168.
  - S. Wang, S. Yang, C. Yang, Z. Li, J. Wang and W. Ge, *J. Phys. Chem. B*, 2000, **104**, 11853.
  - C. Fuentes-Hernandez, J. Thomas, R. Termine, M. Eralp, M. Yamamoto, K. Cammack, K. Matsumoto, S. Barlow, G. Walker, G. Meredith, N. Peyghambarian, B. Kippelen and S. R. Marder, *Proceedings of SPIE-The International Society for Optical Engineering*, 2003, **5216**, 83.
  - S. Wang, Z. Zeng, S. Yang, L. Weng, P. C. L. Wong and K. Ho, *Macromolecules*, 2000, **33**, 3232.
  - L. Daniel, Klayman and T. S. Griffin, *J. Am. Chem. Soc.*, 1973, **95**, 197.
  - S. H. Barbara, *Infrared Spectroscopy: Fundamentals and Applications*, John Wiley & Sons, Incorporated, 2004.
  - K. Surana, P. K. Singh, H. Rhee and B. Bhattacharya, *J. Ind. Eng. Chem.*, 2014, **1**, 19.
  - L. Liu, Q. Peng and Y. Li, *Inorganic Chemistry*, 2008, **47**, 5022.
  - S. Coe, W. Woo, M. Bawendi and V. Bulovic, *Nature*, 2002, **420**, 800.
  - Q. Xin, W. L. Li, G. B. Che, W. M. Su, X.Y. Sun, B. Chu and B. Li, *Appl. Phys. Lett.*, 2006, **89** (22), 223524.
  - C. Li, X. Li, L. Cao, G. Jin and M. Gu, *Appl. Phys. Lett.*, 2013, **102**, 251115.
  - J. R. I. Lee, R. W. Meulenburg, K. M. Hanif, H. Mattoussi and J. E. Klepeis, *PRL*, 2007, **98**, 146803
  - W. W. Yu, L. Qu, W. Guo and X. Peng, *Chem. Mater.*, 2003, **15**, 2854.
  - R. W. Meulenberg, J. R.I. Lee, A. Wolcott, J. Z. Zhang, L. J. Terminello and T. V. Buuren, *A.C.S. NANO*, 2009, **3**, 325.